

FINAL
IN-71-CR
OCT
43775

Prop Rotor Acoustics for Conceptual Design

Final Report
NASA Grant NAG 2-918

Valana L. Wells
Arizona State University

April 1996

Abstract

The report describes a methodology for the simple prediction of noise generated by a tilt-rotor aircraft in hover and forward flight. In order to avoid the computational penalties associated with exact noise calculations, simplifications to the loading noise calculation and the blade-vortex interaction noise calculation have been introduced. The loading noise computation utilizes a constant chordwise loading assumption, while the BVI noise level is estimated through use of a dimensionless parameter, here termed "BVI number." The acoustic computation code, designed as a module for use with VASCOMP, has two modes of operation, one as a quick estimator of acoustic amplitude produced by a tilt rotor with a typical rotor design and the other as a tool for rotor parametric design studies.

1. Introduction

Because of their preliminary success as military transports, tilt-rotor aircraft have become prime candidates for civil use, in particular as a means for efficiently serving the short-haul, city center to city center markets. To fully take advantage of the tilt rotors' capabilities, they should operate in close proximity to businesses and even residences. Probably the largest roadblock to community acceptance of such operations lies in the annoying and possibly extreme noise characteristics of these and virtually any rotary-wing air vehicle. It is anticipated that the Federal Aviation Administration will impose strict acoustic requirements on any proposed commuter tilt-rotor aircraft. To best meet these requirements, tilt-rotor acoustic characteristics, and the effect of overall design strategy on those characteristics, must be addressed at the initial stages of conceptual design.

State-of-the-art methods for evaluating rotor noise signatures have evolved into quite accurate but extremely complicated computer codes. The price for current levels of accuracy is paid in the amount of computer resources necessary for these calculations. Because of the time required for determining the most exact noise level, it is not feasible to use the most modern methods in conceptual design where, perhaps, thousands of possible configurations are evaluated. Therefore, a simpler but still reasonably accurate alternative is necessary for considering acoustic signature in the conceptual design phase.

The current report discusses an acoustic model for evaluating the noise characteristics of tilt-rotor aircraft appropriate for use during conceptual design, and the implementation of the model in the VASCOMP sizing code. Development

of the methodology revolves around the philosophy that, in the initial stages of design, the accuracy of virtually every calculation is known only to within roughly ten percent. It is thus wasted effort to attempt to estimate acoustic properties to within better accuracy than this. Nonetheless, exact theoretical models are utilized for calculation of the acoustic signature produced by rotor-blade thickness and harmonic loading, including “fountain effect” loading. Simplifications to the aerodynamic loading source calculations are implemented. The degree of blade-vortex interaction (BVI) noise is determined in a different and novel manner, through use of a new dimensionless number relating design parameters to the expected amplitude of the BVI acoustic pressure. The model focuses on community noise estimation for a tilt-rotor aircraft in hover and descent since operation in these modes promises to produce the loudest and most annoying acoustic pressures in the surrounding areas. Passenger discomfort caused by high interior noise levels may occur during other flight regimes. This concern is not addressed in the current report, but modifications to the model can be made to also estimate interior noise during high-speed cruise.

2. Acoustic Model Development

For purposes of discussing the computation of tilt-rotor noise, it is convenient to divide the noise constituents into three major categories which include harmonic thickness and loading noise, “fountain-effect” noise, and blade-vortex interaction noise. This categorization is somewhat artificial since fountain-effect and blade-vortex interaction noises are, in fact, types of loading noise. Nevertheless, the description of the components of the acoustics methodology is facilitated by this division.

2.1. Harmonic Noise

The acoustic pressure produced by a surface in relatively low-speed motion is typically divided into terms depending on the surface geometry and motion only (“thickness noise”) and those depending also on the force distribution on the surface (“loading noise”). Since only flight operations near the ground are of concern here, rotor tip Mach numbers are small enough to justify neglecting higher-order, nonlinear propagation effects. The integral equation, developed by Ffowcs Williams and Hawkings, describing thickness and loading noise is utilized for determining the exact thickness and approximate harmonic loading noise.

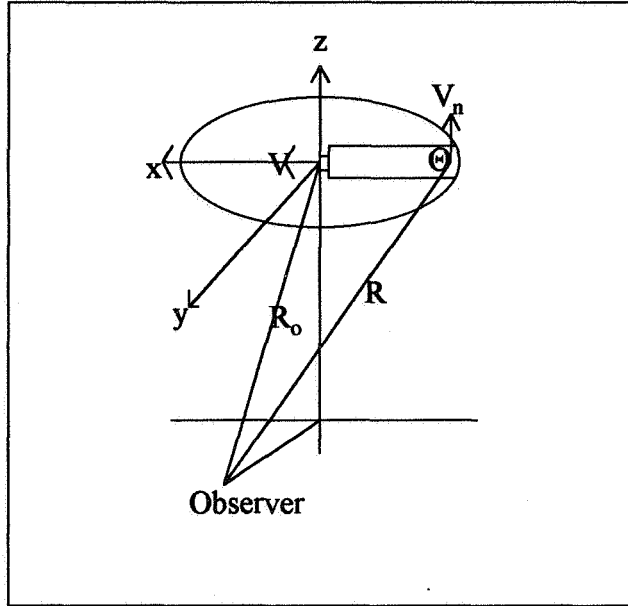


Figure 2.1: Geometry and notation for rotor acoustics

The standard Ffowcs Williams-Hawkins (FWH) equation contains integrals for which the integrands must be determined at the retarded time. The acoustic pressure in the far field can be expressed as:

$$4\pi p' = \frac{\partial}{\partial t} \int \left[\frac{\rho_0 v_n}{R|1 - M_R|} \right] dS + \frac{\partial}{\partial t} \int \left[\frac{p \cos \theta}{R|1 - M_R|} \right] dS \quad (2.1)$$

where the square brackets indicate evaluation at the retarded time, $t - R/c$. The first of the above integrals represents the thickness noise; the second, evaluation of which requires knowledge of the pressure distribution at all points on the surface at all time, describes the loading noise. As illustrated in fig. 2.1, the angle, θ , is the angle between the surface normal and the vector, \mathbf{R} , from a point on the surface to the observer position, R is the length of that vector, and v_n is the velocity normal to the moving surface. Note that if M_R , the Mach number of the surface in the direction of the observer, were to approach 1, the integrands would contain singularities. The conditions of the current problem preclude the achievement of sonic velocity at the rotor tip so that no special treatment of the

singularity is required. The exact thickness noise can be determined relatively easily for a given rotor geometry and motion. To compute loading noise, however, observation of eq. 2.1 indicates that the chordwise as well as the spanwise loading must be provided at all azimuthal locations. Therefore, the acoustics module must have some knowledge of the pressure loading supplied to it in order make a prediction of the loading noise.

Since VASCOMP does not contain a trim procedure, a method, based on that outlined by Prouty[1] was developed for determining required collective and cyclic controls along with the prop-rotor flapping angles. Blade-element calculations then determine the spanwise loading distribution on the blades for a prescribed flight condition. Any combination of forward velocity and climb or descent rates can be accommodated, but most calculations were performed in low-forward-speed descent or hover since these operational conditions generally produce the most noise.

Determining even a simple estimate of the chordwise pressures requires considerable computational resources. A substantial savings in calculation time was realized by making the assumption that, though spanwise loading changes according to the blade-element calculations, the chordwise loading is constant. Thus, for each radial station along the blade, a fictitious, constant Δp , which provides the correct value for the lift per unit span at that location, is computed. The procedure does not eliminate the necessity for chordwise integration in the FWH equation since the values do change for different retarded times. The acoustic calculation itself is, in fact, no less complicated with the constant-loading assumption; the savings arise from the reduction in the complexity of the aerodynamic loading computation.

Figure 2.2 compares the thickness and loading noise using the current method with results computed using an exact method[2] for a trimmed rotor with a tip speed of 650 ft/s. As the figure shows, the loading noise using this simplification compares very well with the more extensive calculation. The degree of accuracy obtained with the simplified method depends on the difference between the actual and assumed loading distributions which, in turn, depends on the trim conditions. Higher tip speed does not necessarily correspond to reduced accuracy for a given set of vehicle parameters since the requirement to trim at a certain thrust will result in a lower required collective for the faster tip. The lower collective may result in a more uniform chordwise loading, offsetting the effects of the higher tip velocity. Figure 2.3 shows a comparison between the approximate and exact thickness and loading noise components for a rotor with tip speed of 800 ft/s.

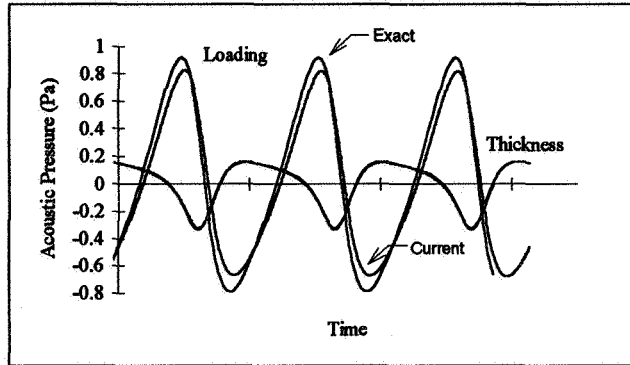


Figure 2.2: Acoustic waveform comparison between current and exact methods, tip speed = 650 ft/s

As expected, both methods predict the same thickness noise. The loading noise, interestingly, compares better at the higher tip speed as a result of the more uniform chordwise loading allowed by the lower collective pitch.

2.2. The Fountain Effect

The noise incurred by the velocity deficit experienced by the rotor blades passing over the wings in hover is sometimes referred to as “fountain effect” noise. The fountain, created by the existence of the wings underneath the rotors, has several important implications in determining the total noise produced by the rotors as illustrated in fig.[3], including the pulses produced by the ingestion into the rotor disk of recirculated turbulence. However, the main deterministic effect can be calculated by allowing a reduction in the inflow velocity during the rotor passage over the wing. This method was first proposed by Rutledge, *et al.*[4], and is implemented in the harmonic loading noise portion of the current model. Figure 2.2 illustrates the directional nature of the “fountain effect” noise. The figure shows the acoustic signatures for a hovering 32,500 lb tilt rotor aircraft with the observer located a distance of 538.5 feet from the center of the rotors and at an angle of 22.5 degrees below the horizontal. For this example, each rotor has three blades with -40° of twist and a taper ratio of .7. Clearly, the fountain-effect noise, characterized by the spike in the pressure waveform, is most prominent behind the aircraft. Though evidence of the fountain effect can be observed at

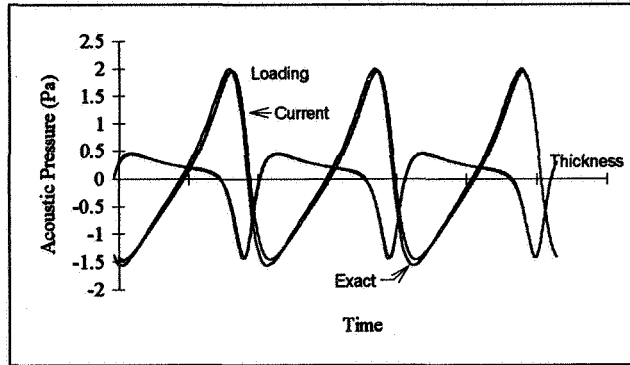


Figure 2.3: Acoustic waveform comparison between current and exact computations, tip speed = 800 ft/s

other azimuthal locations, it appears almost negligible for observers forward of the vehicle.

2.3. Blade-Vortex Interaction Noise

A final component of tilt-rotor noise is that produced by blade-vortex interactions. Evidence suggests that, during flight conditions under which BVI may occur at one nacelle angle, varying the nacelle angle can reduce the severity of the interaction or even eliminate it. Nevertheless, it is desirable to have an estimate of BVI noise level.

Current methods for predicting BVI noise involve three time-consuming steps which include determining the wake location, computing the aerodynamic interference effects of the wake, and using the resulting aerodynamic loading to predict the noise signature. In order to reduce the computational effort in determining the effect of design parameters on BVI noise, a dimensionless number, here termed the “BVI number,” was developed using results from a theoretical blade-vortex interaction study carried out by Hardin[5] in which a relatively simple expression for the acoustic pressure during a parallel interaction is devised. Hardin derives the acoustic pressure under the conditions expressed above as dependent on observer position, circulation strength of the oncoming vortex *and* about the blade at the location of the interaction, the incoming flow speed, the interaction length, and the distance between the vortex and the blade.

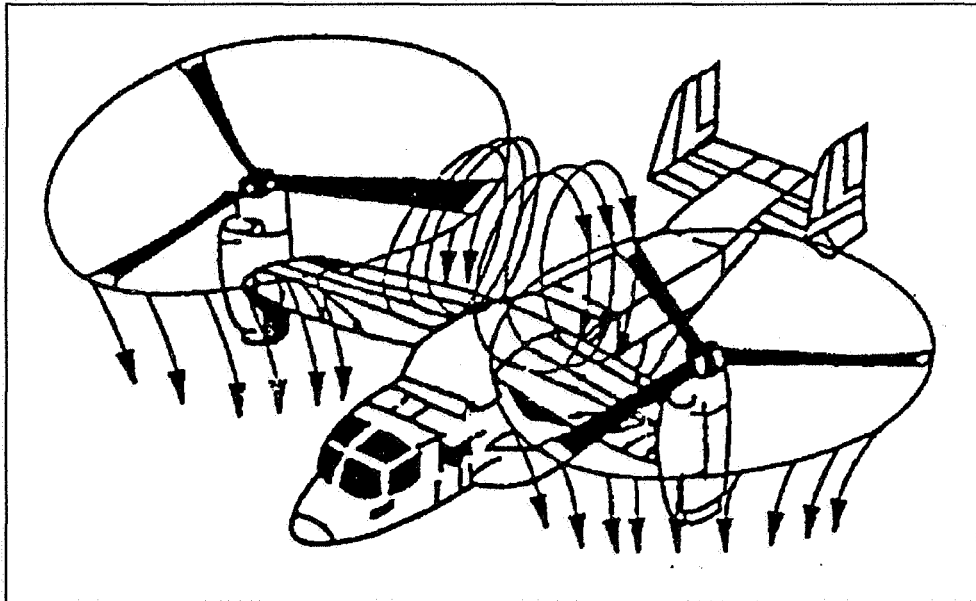


Figure 2.4: Tilt-Rotor Fountain Effect

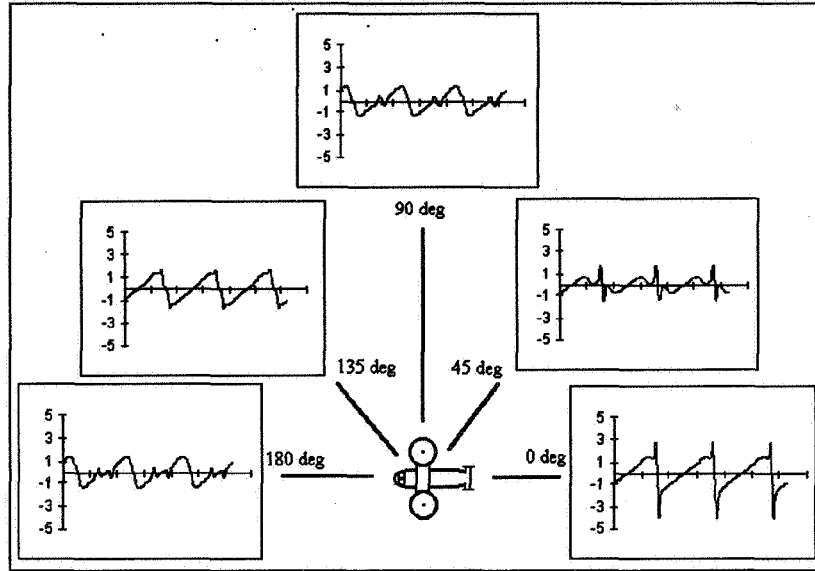


Figure 2.5: Tilt-Rotor Azimuthal Acoustic Directivity

Several parameters, calculated using values known to the VASCOMP program, can be utilized to compute the value of the BVI number. For example, the value of the circulation about the blade at the point of interaction is directly related to the lift coefficient at that location multiplied by the local chord and local velocity. The circulation strength of the traveling vortex depends on the c_l times the chord times the speed near the tip of the rotor at the shedding azimuth. The disk loading, forward speed, and tip-path-plane angle determine the inflow velocity and, thus, an estimate of the vortex miss distance.

Combining the relevant parameters according to their effect as determined by Hardin, the BVI number is defined as

$$\text{BVI}\# = \frac{c_{l_v} c_{l_b} M_{\text{tip}}^3 c_t c_r \sqrt{b} f(\mu)}{r^2}. \quad (2.2)$$

The parameters are defined as follows:

c_{l_w}	lift coefficient at location of vortex generation
c_{l_b}	lift coefficient at location of interaction
c_r	blade root chord
c_t	blade tip chord
M_{tip}	blade tip Mach number
b	number of blades per rotor
μ	advance ratio
r	vertical distance between blade and vortex during interaction

The function $f(\mu)$ accounts for the fact that the number of blade-vortex interactions depends on the advance ratio, as the term, \sqrt{b} , accounts for the influence of the number of blades on the frequency of interactions. Hardin's model does not include these effects since it analyzes only a single BVI event. Clearly, eq. 2.2 can only provide a relative measure of noisiness; it cannot be compared directly with the peak-to-peak acoustic pressures computed for the thickness, loading, and fountain-effect noise.

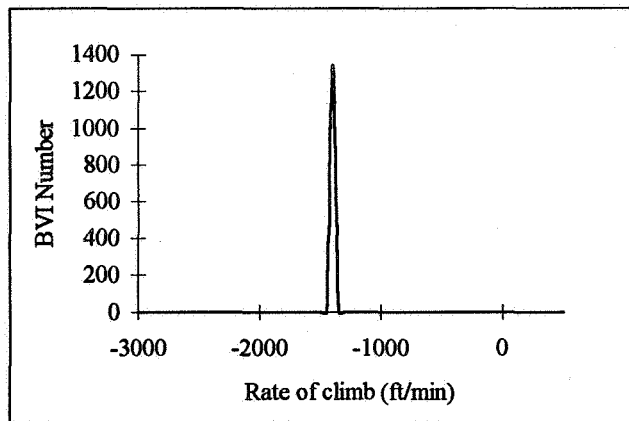


Figure 2.6: BVI number vs climb rate for a typical helicopter with low forward speed.

Based on evaluations for helicopter rotors operating within known BVI regions, a value for this number, above which BVI noise is a likely concern, has been determined. The method does not predict an actual BVI noise level; instead it warns the user of probable high-BVI noise situations. Figure 2.6 shows the value

of the BVI number, as calculated using eq. 2.2, as a function of descent rate for a typical helicopter. The plot clearly identifies the region affected by blade-vortex interactions. Tests indicate that the miss distance, as determined by disk loading, forward velocity, descent rate and trimmed tip-path plane angle, has a larger influence than the other parameters on BVI number.

As long as somewhat conventional rotor planforms are utilized, these and other results indicate that BVI number (and, therefore, BVI noise) is affected as much by operational conditions as by design. The tilt-rotor vehicle, with its greater flexibility in descent configuration, should be able to avoid BVI conditions altogether during normal operations.

3. Example Design Studies

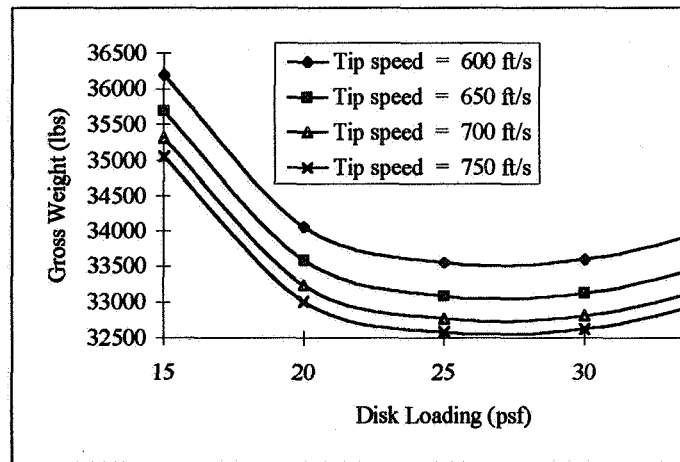


Figure 3.1: Sizing Plot, Wing Loading = 120 ft²

Figure 3.1 shows a typical plot of results from VASCOMP for a civil tilt rotor mission . The aircraft is required to carry 30 passengers 600 N.mi. at a cruise speed of 300 kts. For a wing loading of 120 lb/ft², the minimum-weight aircraft has a disk loading of about 27 lb/ft² and a rotor tip speed of 750 ft/s. As a rule, this would constitute the design point (at least, at the initial, conceptual level) for the given mission.

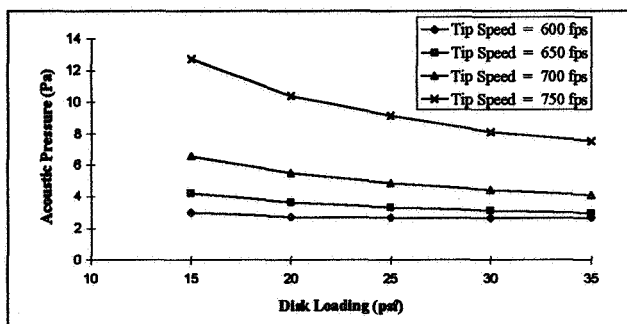


Figure 3.2: Peak-to-peak acoustic pressure, wing loading = 120 psf

The acoustics module can be used to explore alternatives to the initially chosen design point. Figure 3.2 shows, instead of gross weight on the vertical axis, the peak-to-peak acoustic pressure at a chosen observer location for a tilt-rotor aircraft with the same combinations of design parameters as those used in fig. 3.1. For this case, the observer has been located 500 ft in front of the aircraft and 200 ft below, and the vehicle is executing a 540 fpm descent at a forward speed of 100 kt. As expected, the higher tip speeds cause significantly higher acoustic pressure, but the results for various disk loadings exhibit an unexpected trend.

As a general rule, higher pressure loading on the rotor blade surface should produce higher loading noise, with little change in the thickness component. Perhaps surprisingly, fig. 3.2 shows the opposite tendency. Consider the cases of the highest and lowest disk loadings for a single tip speed, for example, 650 ft/s. Sized aircraft under both sets of parameters must meet the specified mission requirements, and must trim to develop the necessary thrust. As indicated by the original sizing plot, the aircraft with the lower disk loading has a higher gross weight, implying that its rotors must generate more thrust. Nonetheless, the rotor with 35 lb/ft² disk loading operates at a considerably higher thrust coefficient than that with a disk loading of 15 lb/ft², with the former at a C_T of 0.0467 and the latter at 0.0211. Again, the higher thrust coefficient would generally indicate higher loading noise because of the stronger loading source. However, because the VASCOMP/Acoustics Module combination considers the many aspects of the design problem, it discovers the somewhat counter-intuitive inclination of the noise, including the loading noise, to decrease as the disk loading increases.

As important to the noise calculation as the source strength is the source

extent. As described by eq. 2.1, the acoustic signal depends on the values of integrals over the rotor blade surface. The smaller rotor, even though it generates more thrust and, thus, higher-magnitude pressure sources, has smaller surface area. The net effect of integrating a stronger source over a smaller area is, in this case, to lessen the total predicted noise. In fact, the loading noise remains a fairly constant function of disk loading with a small decrease in amplitude between 15 lb/ft² and 25 lb/ft², followed by a gradual increase. The thickness noise, which for the selected observer position has approximately the same effect on the total signal, experiences a continuous amplitude decrease as disk loading increases. It should be noted that, for the chosen flight conditions, none of the variable combinations generated a BVI warning.

A goal of low-noise would drive the design to the lowest possible tip speed to minimize both loading and thickness noise. Further examination of fig. 3.1 reveals that by maintaining the disk loading at 27 lb/ft² and reducing the tip speed to 600 ft/s, results in a gross weight increase of approximately 1000 lb. Furthermore, the blade-element aerodynamic analysis shows no indication of blade stall. Obviously, a requirement for a high-g maneuver could preclude the reduction in rotor speed, but, for a civil transport, the small increase in weight may be worth the reduction in noise.

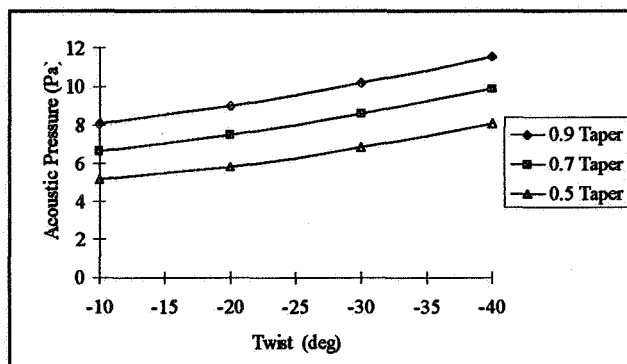


Figure 3.3: Peak-to-peak acoustic pressure, observer located ahead of aircraft, aircraft in forward descent, three-bladed rotors

The acoustics module can be used along with VASCOMP in two different modes. The simplest of these, illustrated by the above results, requires only one call to the acoustics routine per design data point, and default values for blade

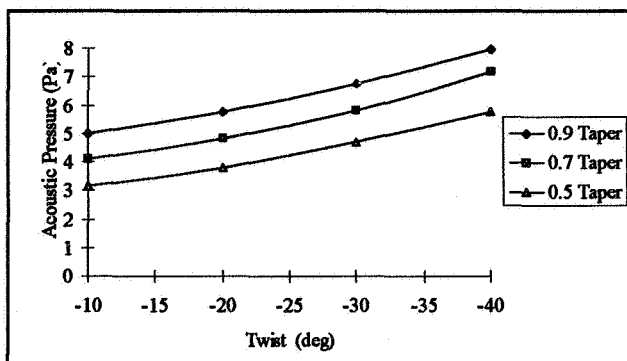


Figure 3.4: Peak-to-peak acoustic pressure, observer located ahead of aircraft, aircraft in forward descent, four-bladed rotors

characteristics are used to estimate the noise for given overall design parameters such as disk loading, wing loading, wing aspect ratio, rotor tip speed, *etc.* All of the above rotor noise values were computed for three-bladed rotors with -30 degrees of twist, and a taper ratio of $.7$. The module can also be used to perform trade-off studies utilizing these rotor characteristics as parameters.

Figure 3.3 shows a plot of the acoustic characteristics of the minimum-weight aircraft in low-speed descent as a function of blade twist and taper. The acoustic results combine thickness noise and harmonic loading noise, and, for this case, the observer is located 500 ft in front of the vehicle and 200 ft below. As expected, increasing the amount of taper, which decreases the blade area near the tip, also reduces the radiated noise. Counter to what might be expected, however, increasing the twist actually increases the predicted noise. Large amounts of rotor twist off-load the rotor tips and, therefore, should reduce the loading noise. However, for all twist values greater in magnitude than -10° , this rotor experiences *negative* loading at the tip on the advancing side. The higher the twist, the greater the negative loading, so that increasing the twist actually has the effect of increasing the outboard lift, albeit negative, resulting in higher peak-to-peak acoustic pressures. Figure 3.4 shows a similar plot of peak-to-peak acoustic pressure as a function of blade twist and taper but for rotors with four instead of three blades. As expected, the noise signal is reduced for rotors with more blades since each blade experiences less severe loading.

4. Conclusions

The acoustics module, developed for use with VASCOMP for conceptual design provides a tool for predicting the noise of tilt-rotor aircraft quickly and, within certain limits, accurately. The code provides an estimate of thickness and loading noise, including the fountain effect in hover. Blade-vortex interaction noise is determined on a relative basis through use of a dimensionless BVI number, developed for use in the acoustics module. Use of the module during the design of an example civil tilt rotor transport has led to several observations:

1. Accounting for acoustic signature during the conceptual design process may lead to the selection of design points different from those chosen using only gross weight as the selection criterion. However, the weight penalty incurred by varying the chosen design parameters may not be substantial, whereas the peak-to-peak acoustic pressure may be considerably reduced.
2. Of all the overall design parameters, reducing tip speed seems to produce the greatest reduction in noise levels, while reducing disk loading can make little difference in the radiated noise. The reduction in tip speed may reduce rotor performance during high-loading maneuvers. Thus, this solution for lowering noise may not be practical for military-attack or other high-performance vehicles.
3. Trends of noise level vs various parameters do not necessarily follow intuitive speculation. The peak-to-peak pressure behaves as expected against tip speed and blade number, but, for the cases tested, the trends vs disk loading and blade twist counter those expected. The module, because it accounts for aspects of the vehicle design (such as trim) rather than varying one parameter at a time, can detect unexpected behavior in the noise trends.
4. The constant-chordwise loading approximation works well for the cases tested. High-collective conditions may reduce the accuracy of the approximation since high blade angle-of-attack will tend to concentrate loading near the airfoil leading edge. High tip speed does not necessarily reduce the accuracy of the model.
5. The BVI number provides some indication of the likelihood of blade-vortex interactions for certain design parameters and flight conditions. However, tilt-rotor aircraft, because of the flexibility afforded them by the ability to

tilt the nacelles, should have the capability of avoiding conditions which cause BVI during normal operations.

The acoustics module does not provide exact values for tilt-rotor acoustic pressure. However, at the conceptual design stage, typical models for aircraft weight, drag, and propulsive characteristics are no more accurate than that provided in the simplified acoustic code. Results from the noise calculations can provide guidance to the designer regarding acoustic trends as functions of design parameters. By including the acoustics module in VASCOMP, some consideration can be given to noise concerns at the early stages of the aircraft design process.

References

- [1] Prouty, R. W., *Helicopter Performance, Stability and Control*. PWS Engineering, 1990.
- [2] Wells, V. L. and Han, A., "Geometrical and numerical considerations in computing advanced-propeller noise," *Journal of Aircraft*, vol. 30, pp. 365-371, May-June 1993.
- [3] George, A. R., Smith, C. A., Maisel, M. D., and Brieger, J. T., "Tilt rotor aircraft aeroacoustics," in *Proc. 45th Annual Forum*, American Helicopter Society, May 1989.
- [4] Rutledge, C. K., Coffen, C. D., and George, A. R., "A comparative analysis of xv-15 tiltrotor hover test data and wopwop predictions incorporating the fountain effect," in *Proceedings of the International Technical Specialists Meeting on Rotorcraft Acoustics and Rotor Fluid Dynamics*, American Helicopter Society and Royal Aeronautical Society, October 1991.
- [5] Hardin, J. C. and Lamkin, S. L., "Concepts for reduction of blade/vortex interaction noise," *Journal of Aircraft*, vol. 24, pp. 120-125, February 1987.